

We Are Never Ever Getting (back to) Ideal Symmetry:

Structure and Luminescence in a Ten-Coordinated Europium(III) Sulfate Crystal

Maria Storm Thomsen, Andy S. Anker, Laura Kacenauskaitė, & Thomas Just Sørensen**

Nano-Science Center and Department of Chemistry, University of Copenhagen,

Universitetsparken 5, 2100 København Ø, Denmark, tjs@chem.ku.dk, mst@chem.ku.dk

Our theoretical treatment of electronic structure in coordination complexes often rests on assumptions of symmetry. Experiments rarely provide fully symmetric systems to study. In solution, fluctuation in solvation, variations in conformation, and even changes in constitution occur and complicate the picture. In crystals, lattice distortion, energy transfer, and phonon quenching is in play, but we are able to identify distinct symmetries. Yet the question remains: How is the real symmetry in a crystal compared to ideal symmetries? Moreover, at what level of detail do we need to study a system to determine, if the electronic structure behaves as if it has ideal symmetry? Here, we have revisited the Continues Shape Measurement (CShM) approach developed by Ruiz-Martínez and Alvarez to evaluate the structure of ten-coordinated europium(III) ions in a $\text{K}_5\text{Na}[\text{Eu}_2(\text{SO}_4)_6]$ structure. By comparing the result of the symmetry deviation analysis to luminescence data, we are able to show the effect of small deviations from ideal symmetry. We suggest using a symmetry deviation value, σ_{ideal} , determined by using our updated approach to Continues Shape Measurements, via our AlignIt code. AlignIt includes normalization and relative orientation in the symmetry comparison, and by combining the calculated values with the experimentally determined energy level splitting, we were able place the first point on a scale that can show how close to ideal an experimental structure actually is.

Europium(III) has 3003 distinct electronic energy levels. Electron-electron repulsion and spin-orbit coupling separates these into 327 groups of states, each described by Russell-Saunders spectroscopic term symbol such as 5D_0 .¹ Each term (group of states) is split by the ligand field into a distinct subset of the 3,003 electronic energy levels.^{2,3}

Among the trivalent lanthanides, Eu(III) is unique as the ground state (7F_0) and the main emitting state (5D_0) both are in a group of states with only a single electronic energy level.^{4,5} This makes the information from optical spectroscopy easier to interpret.^{6,7} Further, the number of the electronic energy levels represented by a spectroscopic term can be directly observed as lines in a high-resolution optical spectrum, see Table 1.^{8,9} This allows for direct observation of system symmetry, which we in this report use to investigate a ten-coordinated Eu(III) complex. First, we determined the degree of structural distortion from the ideal symmetry using our version of the Continuous Shape Measurement (CShM) approach,^{10,11} which we incorporated into the program AlignIt. We then recorded high-resolution optical spectra, and determined the photophysical properties of the Eu(III) ion in this structure. We determined quantum yields, radiative emission lifetimes, line widths, ligand-field splitting and concluded that this crystal structure is a low phonon matrix that allows for high intensity Eu(III) emission. The luminescence lifetime data and the small magnitude of the splitting of states in the 7F_1 term of 28 and 106 cm^{-1} agrees with the designation of high symmetry reported from the single-crystal structural analysis.

The coordination environment surrounding the trivalent ion directly affects optical and electronic properties of lanthanide complexes.¹² In particular, the research field of single-molecule magnetism have sought to exploit the sensitivity of the lanthanide ions

towards ligand coordination to enhance specific properties.¹³⁻¹⁸

Table 1. Number of observable lines in a given $^{2S+1}L_J$ level at different ideal symmetry classes.^{3,19}

$^5D_0 \rightarrow ^7F_J$	Symmetry classes		
	Octagonal	Tetragonal	Ortho-rhombic
	Point groups		
	$D_8, C_{8v},$ S_8, D_{4d}	$D_{4h}, D_4,$ $C_{4h}, C_4,$ D_{2d}, S_4	$D_{2h}, D_2,$ C_{2v}
J = 0	1	1	1
J = 1	2	2	3
J = 2	3	4	5
J = 3	4	5	7
J = 4	6	7	9

It is well established from Laporte's parity selection rules that $4f-4f$ transitions are forbidden, and a decrease in symmetry around the central ion increases orbital mixing and, consequently, increases the probability of transition.^{3,20-22} That is, high symmetry around the lanthanide ion is expected to increase the luminescence lifetime, and – in the absence of quenching – luminescence intensity.³

In the crystal structure of $\text{K}_5\text{Na}[\text{Eu}_2(\text{SO}_4)_6]$, the Eu(III) ion is ten-coordinated by all-oxygen donors. A crystal structure of $\text{K}_5\text{Na}[\text{Ce}_2(\text{SO}_4)_6]$ has been reported by Eriksson *et al.*,²³ in which this conformation is also mentioned as unique for cerium(III) sulfates. Here we present the synthesis, structure, and luminescence properties of $\text{K}_5\text{Na}[\text{Eu}_2(\text{SO}_4)_6]$. In this compound, the Eu(III) coordination geometry can be viewed as a slightly distorted bicapped square antiprism (bcSAP),²⁴ but this description is inadequate for investigating the effect of symmetry on the optical properties. Thus, we calculated deviations of the $\text{Eu}(\text{O})_{10}$ moiety from idealized geometries and other highly

symmetric *f*-element structures in order to evaluate the extent of the distortion from the ideal bicapped square antiprismatic structure. $\text{K}_5\text{Na}[\text{Eu}_2(\text{SO}_4)_6]$ crystallizes in the $C2/m$ space group as rhombohedral blocks. Ten oxygen atoms (see Figure 1) coordinate to the Eu(III) ion. The unit cell contains four Eu(III) ions in dimers of two edge-sharing polyhedra bridged by two sulfate ions (see Figure 1). Crystallographic information is available as supporting information.

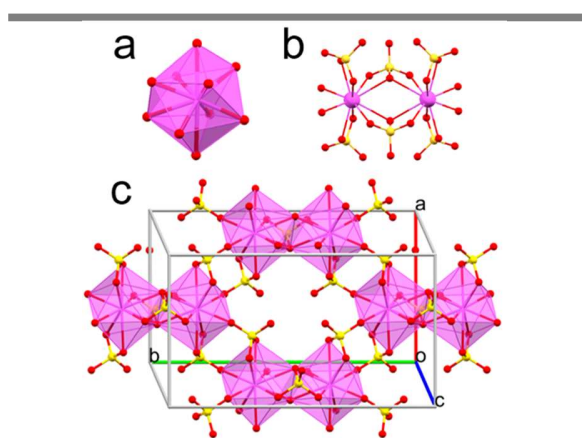


Figure 1 a) Polyhedral illustration of the coordination environment around Eu(III). b) Eu(III) ions in $\text{K}_5\text{Na}[\text{Eu}_2(\text{SO}_4)_6]$ bridged by two sulfate units c) Edge-sharing Eu(III) polyhedra viewed perpendicular to the capping oxygen axis. Eu = pink, O = red, S = yellow. K and Na ions are omitted for clarity.

In order to estimate how close the $\text{Eu}(\text{O})_{10}$ polyhedron is to an ideal bcSAP shape, we applied the Continuous Shape Measures (CShM) approach for ten-coordinated compounds as described by Ruiz-Martínez and Alvarez. The approach is incorporated into the program SHAPE, which is readily available for public use.^{10,11,25} The program calculates a CShM value that describes the degree of shape deviation of a given structure from an ideal structure.

Building on this, we have used a normalization term ($1/N$) to normalize with the number of

atoms in the structure, and a manual pre-alignment of the structures, to verify the optimization before we use equation 1 to calculate the symmetry deviation value, σ_{ideal} .

$$\sigma_{\text{ideal}}(Q) = \frac{\sum_{k=1}^N |Q_k - P_k|^2}{\sum_{k=1}^N |Q_k - Q_0|^2} \cdot \frac{100}{N} \quad \text{eq. (1)}$$

Here Q is the position vector of a ligating atom in the structure, P is the position vector of the corresponding ligating atom in an ideal polyhedron, and Q_0 is the zero point placed in origo.²⁵

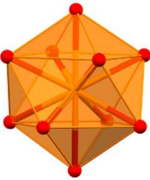



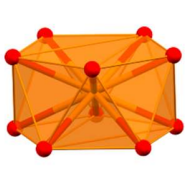
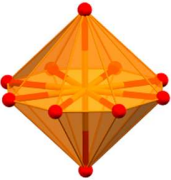
However, to achieve transparent optimization of the intra-atomic distances and rotation in both real and ideal polyhedral, we incorporated equation 1 along with relative orientation and bond length scaling into a program we call AlignIt. Rotational optimization is done through Mercury before using AlignIt. A full description of AlignIt is available in Supporting Information.

Al-Karaghoul and Wood have previously discussed the relative stability of common idealized ten-vertex structures based on calculations of ligand-ligand repulsion energies. Their work revealed that the bicapped square anti-prism (bcSAP) is the most stable ligand arrangement for ten-coordination, closely followed by the bicapped dodecahedron (bcDod) in stability of complexes with coordination number of ten.²⁶ To evaluate deviation from ideal symmetry, we first need to define a scale for our symmetry deviation value, σ_{ideal} , in order to relate the determined value for $\text{K}_5\text{Na}[\text{Eu}_2(\text{SO}_4)_6]$ to ideal symmetries. To generate the scale, we used six ten-vertex ideal polyhedral. The bicapped dodecahedron (bcDod) and the staggered dodecahedron (SDod) are similar in shape to bcSAP, while the pentagonal prism (PP), pentagonal antiprism (PAP) and octagonal bipyramid (OBPy) were selected as shapes that are very different from bcSAP, bcDod and SDod. The

ideal models are spherical idealized, meaning all M-O bond lengths in the structure are equal. The scale only contains ten-vertex polyhedra that to some extent considers ligand-ligand repulsion. Ideal polyhedra that deviates more from bcSAP than PP, PAP and OBP_y exist, but are not included here. Comparative symmetry deviation values, σ_{ideal} , between the ten-vertex polyhedra are shown in Table 2, along with the corresponding CShM values.²⁵ Note that σ_{ideal} values below the diagonal are left out because

they are consistent with the inverse to a second decimal. The full table can be found in Supporting Information. We leave it to the reader to compare the two scales, and only conclude that σ_{ideal} takes values from 0 (identical) to 24 (very different). To test how a non-zero σ_{ideal} value is expressed in terms of physical properties experimental evidence is needed for which we turn to K₅Na[Eu₂(SO₄)₆].

Table 2. Comparative symmetry deviations, σ_{ideal} , for idealized ten-vertex polyhedra^{a,b}

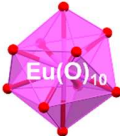


						
	bcSAP <i>D</i> _{4d}	bcDod <i>D</i> ₂	SDod <i>D</i> ₂	PP <i>D</i> _{5h}	PAP <i>D</i> _{5d}	OBPy <i>D</i> _{8h}
bcSAP	0	2.31 (2.30)	7.93 (6.52)	14.46 (13.94)	17.71 (15.52)	16.14 (14.65)
bcDod		0	10.48 (2.13)	16.02 (9.15)	18.76 (8.95)	14.26 (11.75)
SDod			0	17.74 (10.38)	15.93 (6.82)	24.17 (16.83)
PP				0	8.00 (7.85)	22.06 (20.84)
PAP					0	17.27 (16.52)
OBPy						0

^a Coordinates for the SDod, PP, PAP, OBP_y models are reported by Ruiz-Martínez *et al.*¹¹. Coordinates for bcSAP and bcDod were created in Mercury from description by Al-Karaghoulí *et al.*^{26,27} Values in bold are calculated with AlignIt, and values in parenthesis are calculated using SHAPE by Llunell *et al.*²⁵

Using AlignIt to calculate the symmetry deviations for the Eu(O)₁₀ polyhedron in K₅Na[Eu₂(SO₄)₆] we show that it closely resembles the bcSAP geometry. The calculated σ_{ideal} value is shown in Table 3 along two examples that previously have been described as nearly perfect real bcSAP coordination polyhedra, namely thorium(IV) oxalate and uranium(IV) oxalate.^{28,29} The symmetry deviation values of Eu(O)₁₀ in

relation to thorium(IV) oxalate (Th(O)₁₀) and uranium(IV) oxalate (U(O)₁₀) were calculated assuming that the most optimal coordination symmetries for ten-coordination polyhedra are bcSAP, bcDod and SDod.

Table 3. Symmetry deviation values, σ_{ideal} , calculated with AlignIt for ten-vertex polyhedra^{a,b}

	bcSAP D_{4d}	bcDod D_2	SDod D_2
 $\text{Eu}(\text{O})_{10}$	1.15 (1.14)	5.29 (1.47)	7.58 (5.81)
 $\text{Th}(\text{O})_{10}$	0.58 (0.58)	2.63 (2.61)	9.36 (5.44)
 $\text{U}(\text{O})_{10}$	0.53 (0.52)	2.53 (2.53)	9.88 (6.20)

^a Pink polyhedron = $\text{Eu}(\text{O})_{10}$ in $\text{K}_5\text{Na}[\text{Eu}_2(\text{SO}_4)_6]$. Orange polyhedra = Ideal structure models (same as Table 1). Blue polyhedra = $\text{Th}(\text{O})_{10}$, $\text{U}(\text{O})_{10}$. Coordinates for the polyhedra were isolated from the reported crystal structures. The values in parenthesis are CShM values calculated with SHAPE.

$\text{Th}(\text{O})_{10}$ and $\text{U}(\text{O})_{10}$ have high symmetry with a very low $\sigma_{\text{ideal}} < 0.6$ (and CShM) and are thus well represented as bcSAPs. $\text{Eu}(\text{O})_{10}$ has $\sigma_{\text{ideal}}(\text{bcSAP}) = 1.15$, which is slightly higher. Considering the symmetry deviation value of $\sigma_{\text{ideal}}(\text{bcDod}) = 5.29$ and $\sigma_{\text{ideal}}(\text{SDod}) = 7.58$, the structure is clearly best represented by bcSAP. Note that $\text{Th}(\text{O})_{10}$ and $\text{U}(\text{O})_{10}$ also have a low symmetry deviation value from the bcDod structure. Thus, the $\text{Th}(\text{O})_{10}$ and $\text{U}(\text{O})_{10}$ is closely related to bcSAP, with distortions maintaining the similarity to bcDod yet differentiating more towards SDod as a high symmetry deviation value is determined here (see Figure 2). For the $\text{Eu}(\text{O})_{10}$ polyhedron, the case is reversed.

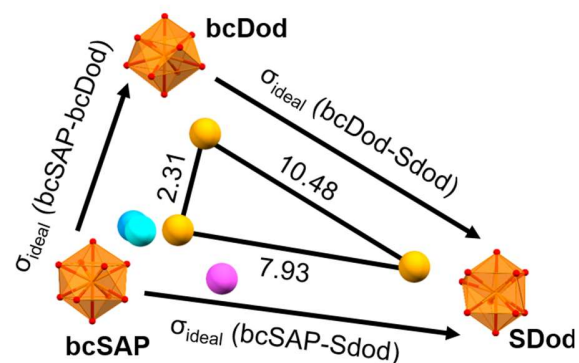


Figure 2 Symmetry deviation relations representing the difference in σ_{ideal} value. Orange spheres = models, blue spheres = $\text{Th}(\text{O})_{10}$, $\text{U}(\text{O})_{10}$ and pink sphere = $\text{Eu}(\text{O})_{10}$.

The symmetry deviation value calculated for $\text{Eu}(\text{O})_{10}$ from $\sigma_{\text{ideal}}(\text{bcDod}) = 5.29$ is higher than that directly between bcSAP and bcDod (2.31), while the symmetry deviation value for $\text{Eu}(\text{O})_{10}$ compared $\sigma_{\text{ideal}}(\text{SDod}) = 7.58$ is lower than the one between bcSAP and SDod (7.93). Thus, we can conclude that the $\text{Eu}(\text{O})_{10}$ polyhedron lies in the space between the bcSAP and the SDod idealized polyhedral (7.93).

The low symmetry deviation value of $\text{Eu}(\text{O})_{10}$ indicates the symmetry around the $\text{Eu}(\text{III})$ ion is close to D_{4d} (bcSAP), with a reduction in symmetry towards D_2 (SDod). We investigated the loss of symmetry via the optical properties of the system at room temperature and 77 K. To evaluate the transition probabilities, the solid state quantum yield of luminescence from $\text{K}_5\text{Na}[\text{Eu}_2(\text{SO}_4)_6]$ was determined to be 38.5 %, with a luminescence lifetime of 2399 μs . Due to lack of an adequate quantum yield reference for solid state measurement, the dye ATTO 390 dissolved in glycerol was used as a reference to mimic the higher refractive index of the crystal compared to aqueous solution (see Supporting Information for details). We note that the procedure is not optimal; however, we considered it the best of the ones available.

The radiative lifetime can be found from eq. 2,

$$\tau_0 = \frac{\tau}{\phi_{Lm}} \quad \text{eq. (2)}$$

Where τ_0 is the radiative lifetime, τ is the observed lifetime of the luminescence and ϕ_{Lm} is the observed luminescence quantum yield. The radiative lifetime for $\text{Eu}(\text{O})_{10}$ in the crystal is determined to $\tau_0 = 6200 \mu\text{s}$ and the rate constant for non-radiative deactivation of the luminescent state is $k_{nr} = 260 \text{ s}^{-1}$ (see supporting information for details). For this low-phonon matrix, the luminescence quantum yield is high and the non-radiative rate constant is low as expected. The highly symmetric nine-coordinated $[\text{Eu}(\text{D}_2\text{O})_9]^{3+}$ complex has a quantum yield of $44 \pm 10 \%$, a $\tau_0 = 3900 \mu\text{s}$ and a $k_{nr} = 140 \text{ s}^{-1}$ in solution.³⁰ The quantum yields and non-radiative rate constants are comparable, however, the radiative lifetime of $\text{Eu}(\text{O})_{10}$ in the crystal is significantly longer than for $[\text{Eu}(\text{D}_2\text{O})_9]^{3+}$, which even considering the higher refractive index of the crystal, indicates an overall higher symmetry environment for $\text{Eu}(\text{III})$ in the crystal than nonaqua coordinated $\text{Eu}(\text{III})$ in solution.

The ligand field perturbation gives rise to the sublevel splitting shown in Table 1. In an ideal bcSAP polyhedron, the central atom will have D_{4d} point group symmetry.²⁶ However, when the emission slit size is decreased it becomes evident that the $^5\text{D}_0 \rightarrow ^7\text{F}_1$ band split into at least three sublevels, as opposed to the two sublevels expected from D_{4d} symmetry (see Figure 4).

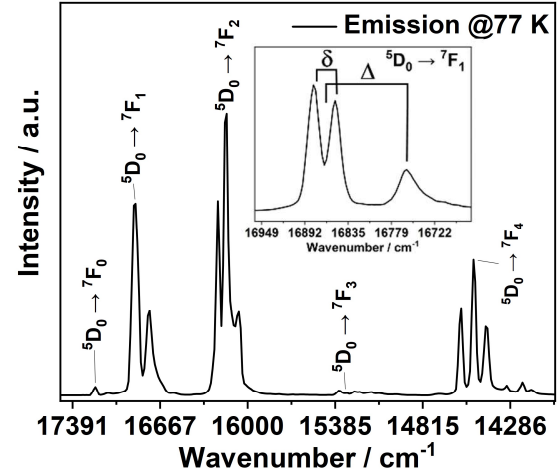


Figure 3. Normalized emission spectrum (ex. 394 nm) of $\text{K}_5\text{Na}[\text{Eu}_2(\text{SO}_4)_6]$ in dimethyl tetrahydrofuran glass at 77K. Emission slit (full spectrum) = 1.5 nm, emission slit ($^5\text{D}_0 \rightarrow ^7\text{F}_1$ transition band) = 1.0 nm

Further resolving the spectra reveals the splitting of the supposedly degenerate $m_J \pm 1$ states.³¹⁻³³ In D_{4d} symmetry, the three $^5\text{D}_0 \rightarrow ^7\text{F}_1$ transitions would be assumed to reduce to two, one from the single state of $^5\text{D}_0$ to the $^7\text{F}_1 m_J = 0$ state, and one from the single state of $^5\text{D}_0$ to the two degenerate $^7\text{F}_1 m_J = \pm 1$ states.^{3,19,34} As three lines clearly are observed, none of the three states described in the $^7\text{F}_1$ term are degenerate.

The local symmetry around $\text{Eu}(\text{III})$ is closely related to the sign of the ligand-field parameters, B_0^2 .³² The ligand-field parameters, B_0^2 and B_2^2 , can proposedly be determined directly from the $^5\text{D}_0 \rightarrow ^7\text{F}_1$ transition band in the emission spectrum by use of eq. 3 and 4.^{32,35,36}

$$\Delta = -\frac{3}{10} B_0^2; \quad \delta = -\frac{\sqrt{6}}{5} B_2^2 \quad (3,4)$$

In axial (e.g. octagonal, tetragonal) symmetry, the B_2^2 parameter is not present as $m_J = \pm 1$ are degenerate. In low symmetry systems, the B_2^2 can easily exceed $150\text{-}200 \text{ cm}^{-1}$.³²

The splitting between the $m_J = \pm 1$, is $\delta = -28 \text{ cm}^{-1}$ (see Figure 4, inset) and between the barycenter of the $m_J = \pm 1$ states and $m_J = 0$ states, is $\Delta = -106 \text{ cm}^{-1}$. The sign of Δ and δ is negative if the $m_J = \pm 1$ states are lower in energy than the $m_J = 0$, corresponding to the $m_J = \pm 1$ states being at higher energies than the $m_J = 0$ in the emission spectrum.^{32,37} Therefore, the ligand field parameters in this formalism are $B_0^2 = 353 \text{ cm}^{-1}$ and $B_2^2 = 57 \text{ cm}^{-1}$. The positive sign of the B_0^2 parameter is a result of an axial contribution to the ligand field potential. The magnitude of the parameters is a direct measure of deviation from symmetry in $\text{Eu}(\text{O})_{10}$, which we compare to $\sigma_{\text{ideal}}(\text{bcSAP}) = 1.15$.

CONCLUSION

The coordination environment around europium(III) in $\text{K}_5\text{Na}[\text{Eu}_2(\text{SO}_4)_6]$ is highly symmetric and closely resembles a bicapped

square antiprism (bcSAP) in geometric shape. To evaluate the deviation from ideality, we present the symmetry deviation value, σ_{ideal} , which builds on the Continuous Shape Measure approach.²⁵ The calculated symmetry deviation value for $\text{K}_5\text{Na}[\text{Eu}_2(\text{SO}_4)_6]$ of $\sigma_{\text{ideal}}(\text{bcSAP}) = 1.15$, which we consider to be low. The symmetry deviation value further allows for assigning the direction of distortion, which in this system is towards a staggered dodecahedron (SDod). The photophysics of the europium(III) centers in the crystal allowed an experimental correlation to the quantitative distortion reflected in the shape deviation. Ligand-field splitting of states in D_{4d} must be symmetric, however, the splitting in the $^7\text{F}_1$ band ($\Delta m_J(\pm 1) = 28 \text{ cm}^{-1}$, $\Delta m_J(\pm 1, 0) = 106 \text{ cm}^{-1}$), and a relative low radiative lifetime ($\tau_0 = 6200 \text{ }\mu\text{s}$) show that the low distortion reported by the symmetry deviation analysis has a significant impact on the physicochemistry of the lanthanide(III) center.

AUTHOR INFORMATION

Corresponding Author

*Thomas Just Sørensen, tjs@chem.ku.dk, @f_elements, Nano-Science Center and Department of Chemistry, University of Copenhagen, Universitetsparken 5, 2100 København Ø, Denmark.

*Maria Storm Thomsen, mst@chem.ku.dk, Nano-Science Center and Department of Chemistry, University of Copenhagen, Universitetsparken 5, 2100 København Ø, Denmark.

Author Contributions

The manuscript was written through contributions of all authors. All authors have given approval to the final version of the manuscript.

Supporting Information

AlignIt program files, AlignIt manual, CIF and CheckCIF files, Example and Input files, Experimental and Crystallographic details, Optical spectra and Diffractograms are available as supporting information.

The Supporting Information is available free of charge on the website.

FUNDING SOURCES

We thank Carlsbergfondet, Villum Fonden (grant#14922), and the University of Copenhagen for funding.

ACKNOWLEDGMENTS

We thank Carlsbergfondet, Villum Fonden (grant#14922), and the University of Copenhagen for support. We thank Villads

Roskjær for help with calculating the bcDod model.

REFERENCES

- (1) Russell, H. N.; Saunders, F. A. New Regularities in the Spectra of the Alkaline Earths. *The Astrophysical Journal* **61**, 38.
- (2) Hänninen, P.; Härmä, H. *Lanthanide Luminescence*; Springer: Heidelberg, 2011.
- (3) Binnemans, K. Interpretation of europium(III) spectra. *Coordination Chemistry Reviews* **2015**, 295, 1.
- (4) Carnall, W. T.; Beitz, J. V.; Crosswhite, H. Electronic energy level and intensity correlations in the spectra of the trivalent actinide aquo ions. III. Bk3+. *The Journal of chemical physics* **1984**, 80 (6), 2301.
- (5) Carnall, W. T.; Goodman, G. L.; Rajnak, K.; Rana, R. S. A systematic analysis of the spectra of the lanthanides doped into single crystal LaF3 *The Journal of chemical physics* **1989**, 90 (7), 3443.
- (6) Kofod, N.; Nawrocki, P.; Juelsholt, M.; Christiansen, T. L.; Jensen, K. M. Ø.; Sørensen, T. J. Solution Structure, Electronic Energy Levels, and Photophysical Properties of [Eu(MeOH)_{n-2m}(NO₃)_m]^{3-m+} Complexes. *Inorganic chemistry* **2020**, 59 (15), 10409.
- (7) Nawrocki, P. R.; Kofod, N.; Juelsholt, M.; Jensen, K. M. Ø.; Sørensen, T. J. The effect of weighted averages when determining the speciation and structure–property relationships of europium(III) dipicolinate complexes. *Physical Chemistry Chemical Physics* **2020**, 22 (22), 12794.
- (8) Binnemans, K.; van Herck, K.; Görlner-Walrand, C. Influence of dipicolinate ligands on the spectroscopic properties of europium(III) in solution. *Chem. Phys. Lett.* **1997**, 266, 297.
- (9) Werts, M. H. V.; Jukes, R. T. F.; Verhoeven, J. W. The emission spectrum and the radiative lifetime of Eu³⁺ in luminescent lanthanide complexes. *Physical Chemistry Chemical Physics* **2002**, 4 (9), 1542.
- (10) Pinsky, M.; Avnir, D. Continuous Symmetry Measures. 5. The Classical Polyhedra. *Inorganic Chemistry* **1998**, 37 (21), 5575.
- (11) Ruiz-Martínez, A.; Alvarez, S. Stereochemistry of Compounds with Coordination Number Ten. *Chemistry – A European Journal* **2009**, 15 (30), 7470.
- (12) Nielsen, L. G.; Junker, A. K. R.; Sørensen, T. J. Composed in the f-block: solution structure and function of kinetically inert lanthanide(III) complexes. *Dalton Transactions* **2018**, 47 (31), 10360.
- (13) Pedersen, K. S.; Dreiser, J.; Weihe, H.; Sibille, R.; Johannesen, H. V.; Sørensen, M. A.; Nielsen, B. E.; Sigrist, M.; Mutka, H.; Rols, S. et al. Design of Single-Molecule Magnets: Insufficiency of the Anisotropy Barrier as the Sole Criterion. *Inorganic Chemistry* **2015**, 54 (15), 7600.
- (14) Perfetti, M.; Sørensen, M. A.; Hansen, U. B.; Bamberger, H.; Lenz, S.; Hallmen, P. P.; Fennell, T.; Simeoni, G. G.; Arauzo, A.; Bartolomé, J. et al. Magnetic Anisotropy Switch: Easy Axis to Easy Plane Conversion and Vice Versa. *Advanced Functional Materials* **2018**, 28 (32), 1801846.
- (15) Konstantatos, A.; Sørensen, M. A.; Bendix, J.; Weihe, H. Lanthanide coordination complexes framed by sodium ions: slow relaxation of the

- magnetization in the Dy(III) derivative. *Dalton Transactions* **2017**, 46 (18), 6024.
- (16) Woodruff, D. N.; Winpenny, R. E. P.; Layfield, R. A. Lanthanide Single-Molecule Magnets. *Chemical Reviews* **2013**, 113 (7), 5110.
- (17) Sessoli, R.; Powell, A. K. Strategies towards single molecule magnets based on lanthanide ions. *Coordination Chemistry Reviews* **2009**, 253 (19), 2328.
- (18) Pedersen, K. S.; Woodruff, D. N.; Bendix, J.; Clérac, R. Experimental aspects of lanthanide single-molecule magnet physics. *Lanthanides and Actinides in Molecular Magnetism* **2015**, 125.
- (19) Tanner, P. A. Some misconceptions concerning the electronic spectra of tri-positive europium and cerium. *Chemical Society Reviews* **2013**, 42 (12), 5090.
- (20) Judd, B. R. Optical Absorption Intensities of Rare-Earth Ions. *Physical Review* **1962**, 127 (3), 750.
- (21) Ofelt, G. S. Intensities of Crystal Spectra of Rare-Earth Ions. *The Journal of Chemical Physics* **1962**, 37 (3), 511.
- (22) Laporte, O.; Meggers, W. F. Some Rules of Spectral Structure*. *J. Opt. Soc. Am.* **1925**, 11 (5), 459.
- (23) Eriksson, A. K.; Casari, B. M.; Langer, V. Pentapotassium sodium hexasulfatodicerate(III). *Acta Crystallographica Section E* **2003**, 59 (11), i149.
- (24) DREW, M. G. B. STRUCTURES OF HIGH COORDINATION COMPLEXES. *Coordination Chemistry Reviews* **1977**, 24 179.
- (25) Llunell, M.; Casanova, D.; Cirera, J.; Alemany, P.; Alvarez, S. SHAPE, version 2.1. *Universitat de Barcelona, Barcelona, Spain* **2013**, 2103.
- (26) Al-Karaghoul, A. R.; Wood, J. S. Crystal and molecular structure of trinitratobis(bipyridyl)lanthanum(III). *Inorganic Chemistry* **1972**, 11 (10), 2293.
- (27) Macrae, C. F.; Sovago, I.; Cottrell, S. J.; Galek, P. T. A.; McCabe, P.; Pidcock, E.; Platings, M.; Shields, G. P.; Stevens, J. S.; Towler, M. et al. Mercury 4.0: from visualization to analysis, design and prediction. *Journal of Applied Crystallography* **2020**, 53 (1), 226.
- (28) Akhtar, M. N.; Smith, A. J. The crystal structure of tetrapotassium tetraoxalatothorium(IV) tetrahydrate, K₄Th(C₂O₄)₄·4H₂O. *Acta Crystallographica Section B* **1975**, 31 (5), 1361.
- (29) Chapelet-Arab, B.; Nowogrocki, G.; Abraham, F.; Grandjean, S. U(IV)/Ln(III) unexpected mixed site in polymetallic oxalato complexes. Part I. Substitution of Ln(III) for U(IV) from the new oxalate (NH₄)₂U₂(C₂O₄)₅·0.7H₂O. *Journal of Solid State Chemistry* **2005**, 178 (10), 3046.
- (30) Kofod, N. A.; Sørensen, T. J. Arel – Investigating Eu(H₂O)₉³⁺ photophysics and creating a method to circumvent luminescence quantum yield determinations. **Submitted**.
- (31) Suturina, E. A.; Mason, K.; Botta, M.; Carniato, F.; Kuprov, I.; Chilton, N. F.; McInnes, E. J. L.; Vonci, M.; Parker, D. Periodic trends and hidden dynamics of magnetic properties in three series of triazacyclononane lanthanide complexes. *Dalton Transactions* **2019**, 48 (23), 8400.
- (32) Parker, D.; Suturina, E. A.; Kuprov, I.; Chilton, N. F. How the Ligand Field in Lanthanide Coordination Complexes Determines Magnetic Susceptibility Anisotropy,

- Paramagnetic NMR Shift, and Relaxation Behavior. *Accounts of Chemical Research* **2020**, 53 (8), 1520.
- (33) Harnden, A. C.; Suturina, E. A.; Batsanov, A. S.; Senanayake, P. K.; Fox, M. A.; Mason, K.; Vonci, M.; McInnes, E. J. L.; Chilton, N. F.; Parker, D. Unravelling the Complexities of Pseudocontact Shift Analysis in Lanthanide Coordination Complexes of Differing Symmetry. *Angewandte Chemie International Edition* **2019**, 58 (30), 10290.
- (34) Hänninen, P.; Härmä, H. *Lanthanide luminescence: photophysical, analytical and biological aspects*; Springer Science & Business Media, 2011.
- (35) Görrler-Walrand, C.; Binnemans, K. In *Handbook on the Physics and Chemistry of Rare Earths*; Elsevier, 1996; Vol. 23.
- (36) Ungur, L.; Chibotaru, L. F. Ab Initio Crystal Field for Lanthanides. *Chemistry – A European Journal* **2017**, 23 (15), 3708.
- (37) Suturina, E. A.; Mason, K.; Geraldes, C. F. G. C.; Kuprov, I.; Parker, D. Beyond Bleaney's Theory: Experimental and Theoretical Analysis of Periodic Trends in Lanthanide-Induced Chemical Shift. *Angewandte Chemie International Edition* **2017**, 56 (40), 12215.

SYNOPSIS

Symmetry deviation analysis is revisited to evaluate the coordination environment in a ten-vertex europium(III) polyhedron in a $\text{K}_5\text{Na}[\text{Eu}_2(\text{SO}_4)_6]$ crystal. After determining the symmetry deviation from ideal polyhedra, the effect of even minor distortions from ideal symmetry is investigated from the splitting of the solid-state luminescence emission of the crystal. The ligand-field perturbation of the energy levels in the lanthanide(III) ion as a results of asymmetry is estimated from the ligand-field parameters.

